An infection-based model of neurodevelopmental damage

Mady Hornig*†, Herbert Weissenböck*‡, Nigel Horscroft*, and W. Ian Lipkin*§

*Emerging Diseases Laboratory, Departments of Microbiology and Molecular Genetics, Anatomy and Neurobiology, and Neurology, University of California, Irvine, CA 92697-4292; †Department of Psychiatry, University of Pennsylvania, Philadelphia, PA 19104-2649; and ‡Institute for Pathology and Forensic Veterinary Medicine, University of Veterinary Medicine, Vienna A-1210, Austria

Communicated by James L. McGaugh, University of California, Irvine, CA, August 19, 1999 (received for review June 9, 1999)

Perinatal exposure to infectious agents and toxins is linked to the pathogenesis of neuropsychiatric disorders, but the mechanisms by which environmental triggers interact with developing immune and neural elements to create neurodevelopmental disturbances are poorly understood. We describe a model for investigating disorders of central nervous system development based on neonatal rat infection with Borna disease virus, a neurotropic noncytolytic RNA virus. Infection results in abnormal righting reflexes, hyperactivity, inhibition of open-field exploration, and stereotypic behaviors. Architecture is markedly disrupted in hippocampus and cerebellum, with reduction in granule and Purkinje cell numbers. Neurons are lost predominantly by apoptosis, as supported by increased mRNA levels for pro-apoptotic products (Fas, caspase-1), decreased mRNA levels for the anti-apoptotic bcl-x, and *in situ* labeling of fragmented DNA. Although inflammatory infiltrates are observed transiently in frontal cortex, glial activation (microgliosis > astrocytosis) is prominent throughout the brain and persists for several weeks in concert with increased levels of proinflammatory cytokine mRNAs (interleukins 1α, 1β, and 6 and tumor necrosis factor α) and progressive hippocampal and cerebellar damage. The resemblance of these functional and neuropathologic abnormalities to human neurodevelopmental disorders suggests the utility of this model for defining cellular, biochemical, histologic, and functional outcomes of interactions of environmental influences with the developing central nervous system.

Intrauterine or perinatal exposures to infectious, immune, or other environmental factors are proposed as primary mediators of central nervous system (CNS) damage in neuropsychiatric syndromes (1–4). Identification of neuropathologic events after perinatal injury and description of their functional correlates are required to understand the mechanisms by which environmental triggers interact with developing immune and neural elements and the pathogenic basis of neurodevelopmental disorders.

Borna disease virus (BDV), an atypical, neurotropic, noncytolytic, negative-strand RNA virus, is tropic for limbic and cerebellar circuitry. Infection causes a spectrum of behavioral deficits depending on the age, immune status, CNS maturity, and genetics of the host. In immunocompetent adult Lewis rats, infection results in meningoencephalitis, diffuse CNS damage, dopamine neurotransmitter disturbances, and disorders of movement and behavior (5). Neonatally infected rats are reported not to have inflammation (6–10) but nonetheless have abnormalities of hippocampal and cerebellar development (6), growth (9), play behavior (10), and learning (11, 12) that correlate with disturbances observed in some children with autism.

Autism spectrum disorders occur as frequently as 1 in 500 children (13, 14), a rate that may be increasing in some geographic regions (13). A neurodevelopmental hypothesis for autism is supported by neuroimaging (15), anatomic and cytoarchitechtonic (16, 17), and epidemiologic (18) findings. However, no established animal model for autism addresses the following: its likely perinatal origins (17); linkage to microbial (19, 20) or immune factors (21); association with hippocampal, amygdaloid, and cerebellar dysfunction (17); connection with dopamine, serotonin, and other neurochemical disturbances (22); and variable neurobehavioral derangements (motor, postural, and sensory deficits; hypotonia; stereotypies; poor eye contact; mental retardation; islands of normal to supernormal functioning) superimposed on impairments in social interaction, communication, and behavior (14).

Here we describe a model of neurodevelopmental damage after neonatal BDV infection of Lewis rats wherein disturbances of CNS architecture and function parallel the structural and behavioral abnormalities observed in autism. These abnormalities are accompanied by shifts in soluble factors (cytokines, apoptosis-related products, neurotrophic factors). This model suggests mechanisms by which environmental influences can injure specific neural elements during critical periods of nervous and immune system development, and may provide insights into the pathogenesis of autism and other neurodevelopmental disorders.

Materials and Methods

Animals. Lewis rat pups (Charles River Breeding Laboratories) were inoculated intracerebrally within 12 h of birth with 50 μl of 5×10^3 tissue culture infectious units of BDV strain He/80–1 (23) (NBD rats) or normal rat brain homogenate or PBS (NL rats). Rats were tested in behavioral paradigms at days 4, 7, and 9 post inoculation (p.i.), or at 4, 6, 12, 24, or 52 wk p.i., or they were sacrificed for brain dissection at 2, 3, 4, 5, 6, 12, 24, or 76 wk p.i.

Assessments of Clinical Status and Early Developmental Milestones. Clinical parameters rated by observers blind to experimental group during three 10-sec observation periods, 30 min apart, included the following: disheveled fur, lethargy, paresis, or dystonia (score of 0, no disturbance; 0.5, minimal to mild disturbance; 1, moderate to severe disturbance; maximum score of 4 per observation period). Developmental and motor changes assessed were weight, protoambulatory responses (falls while ambulating, number of grid cells crossed), and negative geotaxis (latency to turning head 75° or more uphill when placed head down on a 25° inclined plane) (24). Changes in development and motor coordination were tested by measurement of weight, gait, and dowel-walking (length of time the animal remained on a 0.5-inch (1.3-cm)-diameter fixed dowel during a 30-sec test).

Behavioral Studies. Locomotor activity was quantified by using activity chambers (5). Stereotypies were independently assessed by two experienced raters using a standardized rating scale (5, 25).

Histology and Immunohistochemistry. Anesthetized rats (methoxyflurane) were perfused with 4% buffered paraformaldehyde. After postfixation and cryoprotection of brains in sucrose, 20-μm serial coronal cryostat sections of frontal and olfactory cortex (Cx); striatum; nucleus accumbens; parietal, temporal,

Abbreviations: CNS, central nervous system; BDV, Borna disease virus; NBD, neonatal Borna disease; p.i., post inoculation; Cx, cortex; Hc, hippocampus; DG, dentate gyrus; Amyg, amygdala; Cblm, cerebellum; TUNEL, terminal deoxynucleotidyltransferase dUTP-biotin nick end labeling; RPA, RNase-protection assay; TNF, tumor necrosis factor.

§To whom reprint requests should be addressed. E-mail: ilipkin@uci.edu.

The publication costs of this article were defrayed in part by page charge payment. This article must therefore be hereby marked "*advertisement*" in accordance with 18 U.S.C. §1734 solely to indicate this fact.

and occipital Cx; thalamus and hypothalamus; hippocampus (Hc); amygdala (Amyg); midbrain; medulla; and cerebellum (Cblm) were collected on coated slides (Vector Laboratories).

Tissue sections were stained with hematoxylin and eosin for histology. Immunohistochemistry was performed with the following: rabbit anti-BDV nucleoprotein (N; 1:5000 dilution); rabbit anti-glial fibrillary acidic protein (GFAP; 1:1000 dilution; Dako); rabbit anti-inducible nitric oxide synthase (iNOS; 1:500 dilution; Transduction Laboratories); and goat anti-rat IgG (1:100 dilution; Vector Laboratories). Immune cell markers were detected (26) by using monoclonal antibodies: OX19 (CD5, pan-T cell marker), W3/25 ($CD4^+$ T cell marker), OX8 ($CD8^+$ T cell marker), 3.2.3 (natural killer cell marker), and OX42 (macrophage and activated microglial cell complement receptor type 3 marker; gift of W. F. Hickey, Dartmouth Medical School, Hanover, NH). Secondary antibodies were biotinylated anti-rabbit IgG (1:200 dilution) or biotinylated anti-mouse IgG (rat absorbed) (1:100 dilution) (Vector Laboratories). Antibody binding was visualized using a Vectastain ABC kit (Vector Laboratories) with diaminobenzidine as chromogen. Relative binding of antibodies on immunohistochemical measures was scored on a scale from 0 (none) to 3+ (strong) in meninges, cerebral vessels, and parenchyma.

Terminal Deoxynucleotidyltransferase (TdT) dUTP-Biotin Nick End Labeling (TUNEL). Cells with fragmented DNA were labeled by TUNEL with diaminobenzidine as chromogen (27). Positive cells (brown nuclear staining) were counted in five randomly selected fields at 200× magnification and were classified as meningeal, parenchymal, or perivascular in distribution in frontal Cx, olfactory Cx, Hc, Amyg, Cblm, striatum, thalamus, and hypothalamus.

RNase-Protection Assay (RPA). Anesthetized NBD and NL rats were decapitated. Using defined coordinates (28), prefrontal Cx, nucleus accumbens, Hc, Amyg, and Cblm were dissected on ice; RNA was extracted with TriReagent (29). A multiprobe RPA system (PharMingen) was used to quantitate transcripts corresponding to mRNAs encoding cytokines, neurotrophic factors, and apoptosis-related products; L32 and glyceraldehyde-3-phosphate dehydrogenase (GAPDH) served as control probes. Panels were cytokines, interleukin (IL)1α, IL1β, IL2, IL3, IL4, IL5, IL6, IL10, tumor necrosis factor (TNF)α, TNFβ, and interferon (IFN)γ; neurotrophic factors, βNGF, BDNF, GDNF, CNTF, NT3, and NT4; apoptosis-related products, Fas, FasL, caspase-1, caspase-3, caspase-2(L/S), bax, bcl-x(L/S), and bcl-2. Protected fragments were resolved on a denaturing 5% acrylamide gel and visualized by phosphorimaging (Molecular Dynamics). Transcript levels were quantitated by normalization to control probes with IQMAC software (Molecular Dynamics).

***In Situ* Hybridization for BDV Genomic RNA.** Brain sections were hybridized with an ^{35}S-labeled RNA probe (specific activity $2–6 \times 10^7$ cpm/μg; 5 ng of probe per slide) complementary to BDV genomic RNA (30).

Statistical Analysis. Analyses were performed with STATVIEW v5.0.1 (SAS Institute). Tests for homogeneity of variance were performed on early motor responses (number of grid cells crossed, latency of geotaxis), locomotor activity scores (crossovers), and stereotypy ratings. Two-way analysis of variance (ANOVA) with groups (NBD, NL) and wk p.i. (4, 6, 12) as independent factors ($\alpha = 0.05$) was used to compare mean clinical scores (±SEM) and mean crossovers per 30-min testing period (±SEM). Repeated measures ANOVA was used to assess changes in locomotor activity across the three 30-min observation periods, using group membership and time p.i. as independent factors, and time as the repeated measure. Group means for weight, number of grid cells entered, and geotactic response latencies were compared using two-way ANOVA, with group membership (NBD, NL) and age p.i. (days 4, 7, 9) as independent factors. For all ANOVAs, subsequent individual means comparisons were analyzed by using post hoc Fisher's protected least significant difference (PLSD) tests with $\alpha = 0.05$ (31). Where assumptions of homogeneity of variance were violated, differences between groups were compared by nonparametric Mann–Whitney U tests ($\alpha = 0.05$) (32). χ^2 analysis (two-tailed) was used to assess differences in motor function (falling onto back) between groups ($\alpha = 0.05$). Group and time-point effects for cytokines, neurotrophic factors, and apoptosis-related proteins were examined in each brain region by two-way ANOVA with post hoc Fisher's PLSD tests ($\alpha = 0.05$) for subsequent individual means comparisons.

Results

Clinical Characteristics of NBD Rats. None of the NBD rats had classic Borna disease or meningoencephalitis. Clinical assessments revealed a significant overall difference between NBD and NL groups ($P < 0.0001$); subsequent individual means comparisons revealed small but significant differences at 4 and 12, but not 6 wk (mean ± SEM at 4 wk: NBD, 0.58 ± 0.21 vs. NL, 0.01 ± 0.01, $P = 0.0034$; 6 wk: NBD, 0.06 ± 0.03 vs. NL, 0.19 ± 0.08, P = not significant; 12 wk: NBD, 0.99 ± 0.11 vs. NL 0 ± 0, $P < 0.0001$). Clinical scores for NBD rats at 24 and 52 wk ($n = 4$ per group) were 1.21 ± 0.13 and 0.88 ± 0.13, respectively.

Abnormalities of Early Development. Delays in growth and maturation were evident as early as day 4 p.i. NBD rats weighed less than NL rats at day 4 (two-way ANOVA, $P < 0.0001$; day 4 weights: NBD, 9.9 ± 0.4 g vs. NL, 11.8 ± 0.1 g, $P < 0.0001$). Growth delays were progressive through wk 24 (NBD, $n = 8$: 276.1 ± 12.5 g vs. NL, $n = 2$: 437 ± 0 g; $P = 0.0003$). NBD rats had asymmetric protoambulatory responses, with falls into a supine position. These locomotor abnormalities were present in 3 of 10 NBD rats at day 4 p.i. ($P = 0.007$), 4 of 10 NBD rats at day 7 ($P = 0.0015$), but faded to 1 of 10 NBD rats at day 9 (P = not significant), and were not observed in controls (0/22; overall $\chi^2 = 19.2$, $P < 0.0001$). Righting responses were delayed up to 3 sec (24). Distance traveled in the open-field chamber was also decreased in NBD rats (Fig. 1).

NBD and NL rats did not differ in another developmental reflex, the negative geotactic response (mean latency: NBD, 14.3 ± 1.9 sec; NL, 18.4 ± 3.3 sec; P = not significant, Mann–Whitney U test).

Cerebellar Dysfunction. One of 15 NBD rats had mild gait ataxia at 12 wk. None of 4 NBD rats had gait disturbance at 24 wk p.i.; however, all 52 wk rats ($n = 4$) were moderately ataxic with

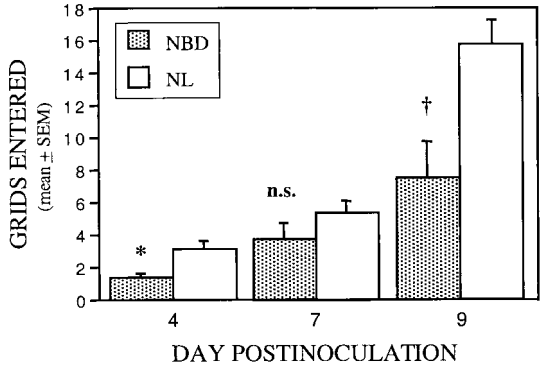

Fig. 1. Early locomotor activity after neonatal BDV infection. Grid cell crossings in open-field chamber (2-min test) at days 4, 7, and 9 p.i. in infected (NBD; $n = 10$) vs. normal (NL; $n = 22$) rats. Two-way ANOVA, $P = 0.0003$. *, $P = 0.02$; n.s., not significant; †, $P = 0.005$.

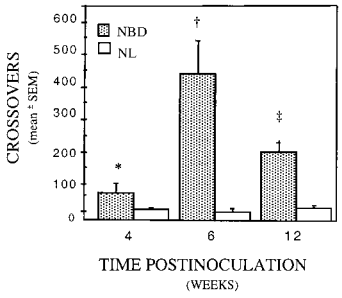

Fig. 2. Hyperactivity at 4, 6, and 12 wk p.i. Serial changes in locomotor activity (mean crossovers ± SEM) in infected (NBD) and uninfected (NL) rats (n = 4–9 per group). ∗, $P = 0.029$; †, $P = 0.001$; ‡, $P = 0.0009$ (NBD vs. NL).

intermittent "hopping gait" and mild hindpaw spasticity. All NL rats had normal gait. At 12 wk, NBD rats remained on the dowel for an average of 3.0 ± 2.4 sec ($n = 6$); at 24 ($n = 4$) and 76 wk ($n = 4$), rats immediately fell off the dowel. All NL rats (12 and 24 wk; $n = 4$ per group) remained on the dowel for 30 sec.

Locomotor Activity and Response to Novel Environment. Locomotor activity was increased in NBD rats at all time points. Six-week NBD rats had the greatest increases in overall mean crossover activity relative to NL (Fig. 2; two-way ANOVA, Group effect: $P < 0.0001$; Group × Week effect: $P = 0.003$).

Exploratory behavior patterns and adaptation to novel environment were assessed by comparing changes in mean activity across a 90-min testing session (Table 1). At 4 wk, NBD rats had prolonged locomotor inhibition upon introduction to the novel environment (0–30 min) (repeated measures ANOVA, Group effect: $P = 0.029$; Crossovers × Time × Group interaction effect: $P < 0.0001$). Over subsequent intervals (30–60 min, 60–90 min), 4-wk NBD rats were hyperactive.

Subtle Increase in Stereotypies in NBD. Sniffing and rearing behaviors were increased in NBD rats. Median stereotypy ratings were higher for NBD than NL rats at 4 wk ($P = 0.02$), 6 wk ($P < 0.0001$), and 12 wk ($P = 0.02$): the median rating for NBD rats was 4 at all time points (range 0–5); the median rating for NL rats was 3 (range 0–4) at 4 wk, 0 (range 0–5) at 6 wk, and 3 (range 0–4) at 12 wk.

Regional and Developmental Shifts in Soluble Factor Gene Expression. Transcripts corresponding to mRNAs for IL1α, IL1β, IL6, and TNFα were significantly increased in the majority of brain regions tested in NBD rats, beginning at wk 4 p.i. (Fig. 3). TNFβ mRNA was increased at wk 6 in Cblm of NBD rats (4,100 ± 376 in NBD vs. 1,600 ± 470 in NL, $P = 0.0142$), but declined to levels below control values by wk 12 (3 ± 3 in NBD vs. 287 ± 72 in NL, $P = 0.0135$). TNFβ mRNA levels were also significantly lower at 6 wk p.i. in prefrontal Cx (3,324 ± 632 in NBD vs. 11,413 ± 428 in NL, $P = 0.0004$) and at 2 and 4 wk in pooled Amyg samples (overall $P = 0.0094$; 2-wk values: 45 in NBD, 569 in NL; 4-wk values: 129 in NBD,

Table 1. Adaptation to novel environment in NBD rats at 4 wk p.i.

	Crossovers		
Group	0–30 min	30–60 min	60–90 min
NBD	21.5 ± 3.6*	80.8 ± 30.8†	151.2 ± 60.2‡
NL	63.9 ± 7.3	13.8 ± 6.7	16.8 ± 6.2

Number of crossovers during successive 30-min testing sessions are presented as mean ± SEM. *, $P = 0.003$; †, $P = 0.015$; ‡, $P = 0.0087$ (4-wk NBD vs. 4-wk NL rats).

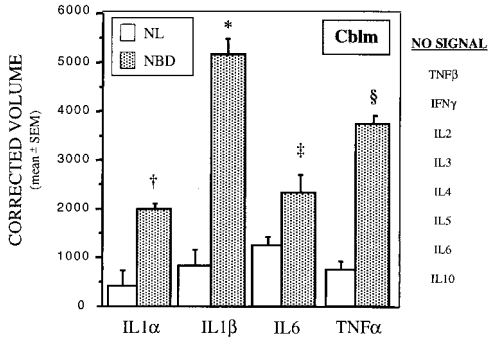

Fig. 3. Cytokine gene expression in infected (NBD) and uninfected (NL) Cblm at 4 wk p.i. Values of mRNA for cytokines on RPA analysis are normalized to L32 mRNA levels (n = 3 per group). †, $P = 0.0043$; ∗, $P = 0.0007$; ‡, $P = 0.0024$; §, $P = 0.0004$ (NBD vs. NL).

535 in NL). Levels of mRNAs for proinflammatory cytokines, IL2, IL3, and IFNγ, and Th_2-type cytokines, IL4, IL5, and IL10, were similar in NBD and NL rats at all time points.

Alterations in transcripts encoding genes associated with regulation of apoptosis appeared at 2 wk p.i. and persisted through wk 12. Whereas levels of mRNAs for FAS and caspase-1, two promoters of apoptosis, were increased throughout the brain from 4 wk p.i., mRNA for bcl-x(L), a neuroprotective factor that inhibits apoptosis, was decreased only in Hc (Fig. 4) and Cblm (data not shown). In Hc, this decrease in bcl-x(L) mRNA occurred at wk 2 (NBD vs. NL: 175,396 ± 4,541 vs. 296,102 ± 23,257; $P = 0.007$) and wk 4 p.i.; in Cblm, bcl-x(L) mRNA values were decreased only at 6 wk (NBD vs. NL: 62,730 ± 1,406 vs. 80,559 ± 4,506; $P = 0.019$). At later time points (wk 12) increases in normalized mRNA values for the anti-apoptotic product bcl-2 were noted in Hc (NBD vs. NL: 51,015 ± 5,124 vs. 28,339 ± 3,925; $P = 0.025$) and Cblm (NBD vs. NL: 11,961 ± 1,105 vs. 5,566 ± 1,749; $P = 0.037$). RPA signals in NBD and NL rats were similar for caspase-3 or bax, pro-apoptotic products expressed constitutively in brain (33).

Shifts in neurotrophic factor transcripts were present only in Hc. BDNF, βNGF, and NT3 first declined in Hc of NBD rats at 4 wk, but the decline did not achieve statistical significance until 12 wk p.i. (Fig. 5; two-way ANOVA, Group effect: $P < 0.0001$). Apparent differences in gene expression for CNTF between NBD and NL groups did not achieve statistical significance. NT4 and GDNF were not detected.

Cerebral Atrophy and Cell Loss in NBD. Whole brain mass decreased between 2 and 24 wk. Prominent findings were neuronal loss in cerebral Cx, dentate gyrus (DG), Purkinje cell layer of Cblm (Fig. 6*)*, deep cerebellar nucleus, ventral cochlear nucleus, and

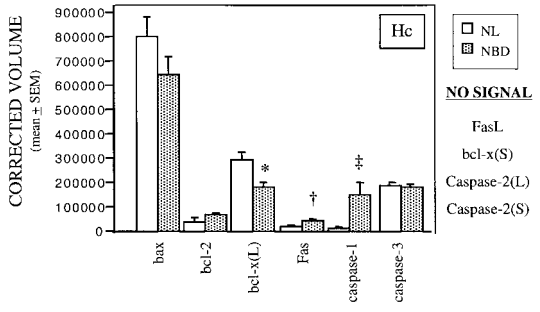

Fig. 4. Apoptosis-related gene expression in infected (NBD) and uninfected (NL) Hc at 4 wk p.i. Values of mRNA for apoptosis-related products on RPA are normalized to L32 mRNA levels (n = 3 per group). ∗, $P = 0.03$; †, $P = 0.017$; ‡, $P = 0.04$.

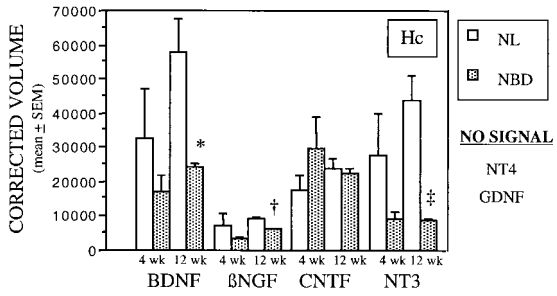

Fig. 5. Neurotrophic factor gene expression in infected (NBD) and uninfected (NL) Hc at 4 and 12 wk p.i. Values of neurotrophic factor mRNA from RPA analysis are normalized to L32 mRNA levels ($n = 3$ per group). BDNF, brain-derived neurotrophic factor; βNGF, β nerve growth factor; CNTF, ciliary neurotrophic factor; NT3, and NT4, neurotrophins 3 and 4; GDNF, glial cell line-derived neurotrophic factor. *, $P = 0.013$; †, $P = 0.0015$; ‡, $P = 0.008$.

superior colliculus. These lesions were first visible at 3 wk, peaked at 4 wk, and continued through 6 wk p.i. Atrophy of DG was progressive from 5 wk p.i. At 6 wk, glial cells replaced granule cells (microgliosis > astrocytosis; Fig. 7 *A–D*). Purkinje cells were depleted beginning at wk 4 and continuing to wk 24. Architecture of Cblm was retained despite marked reduction in thickness of cell layers; no ectopic cells nor other signs of developmental arrest were seen.

Astrocytosis and microgliosis were evident in all brain regions by 3 wk p.i. (Fig. 7). The onset and distribution of glial cell proliferation coincided with neuronal loss yet was sustained through 24 wk p.i., after neuronal cell death waned. Astrocyte and microglia morphology was consistent with activation (increased cytoplasm; short, thickened processes; additionally, in microglia, more intense staining with OX42). In Hc, gliosis was most evident in DG. In Cblm, gliosis was equally prominent in white and gray matter. Microgliosis persisted throughout the brain as late as 76 wk p.i.

Moderate to severe mononuclear infiltration of meninges and neuroparenchyma was found in cingulate, retrosplenial, frontal, parietal, temporal, and occipital Cx beginning at 4 wk p.i. (Fig. 7*E*). Infiltrating inflammatory cells were rare in Hc, Cblm, mesencephalon, and brainstem. Perivascular cuffs consisted primarily of T lymphocytes. Activated microglial cells were abundant in adjacent neuropil. Inflammatory infiltrates decreased by 5 wk and resolved by 6 wk p.i.

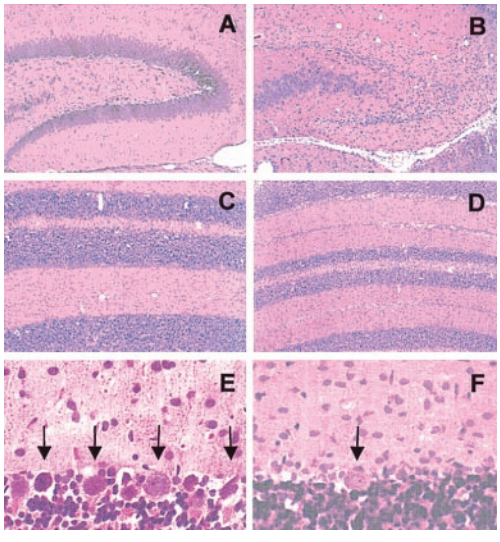

Fig. 6. (*A* and *B*) Dentate gyrus in uninfected (*A*) and neonatally infected (*B*) rats at 5 wk p.i. (Hematoxylin and eosin; ×20.) (*C–F*) Cerebellar atrophy and Purkinje cell loss at 4 wk p.i. (Hematoxylin and eosin; *C* and *D*, ×20; *E* and *F*, ×120.) Cblm from uninfected (*C* and *E*) and infected (*D* and *F*) rats. Arrows in *E* and *F* indicate Purkinje cells.

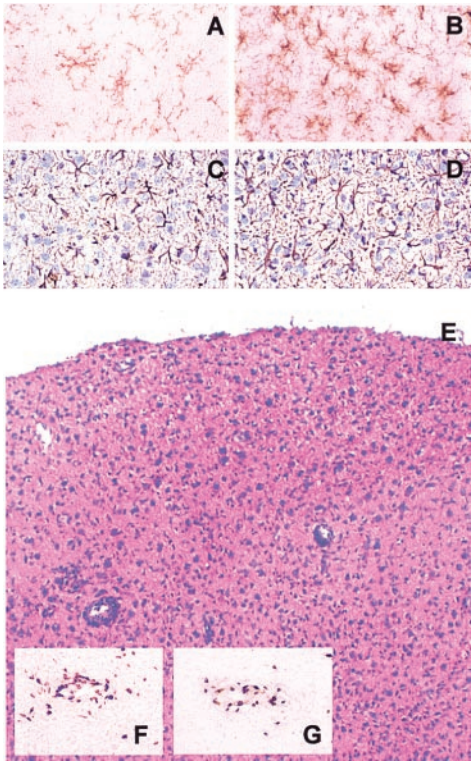

Fig. 7. (*A–D*) Microgliosis and astrocytosis at 6 wk p.i. in rat mesencephalon (*A* and *B*) and parietal Cx (*C* and *D*). Anti-OX42 staining of microglia (*A*, uninfected; *B*, infected); anti-glial fibrillary acidic protein (GFAP) staining of astrocytes (*C*, uninfected; *D*, infected). (×80.) (*E–G*) Transient T cell response in parietal Cx of infected rats at 4 wk p.i. (*E*, hematoxylin and eosin; ×36. *F*, W3/25 staining for CD4, ×50. *G*, OX8 staining for CD8, ×50.)

Immune Cell Marker Immunoreactivity. Inflammatory cells consisted chiefly of T cells (OX19; data not shown). T cells were present in leptomeninges, perivascular cuffs, and neuropil. $CD4^+$ (W3/25; Fig. 7*F*) and $CD8^+$ (OX8; Fig. 7*G*) T cells were found in nearly equal numbers. $CD4^+$ T cells were predominantly confined to perivascular spaces and leptomeninges, whereas $CD8^+$ T cells were more numerous in neuropil. Single natural killer cells (3.2.3 marker; data not shown) were present in perivascular cuffs and neuropil.

Inducible NO Synthase (iNOS) Immunohistochemistry. Immunoreactivity of iNOS was found only in Cx of rats at 4 to 5 wk p.i. and localized to single macrophages in neuropil, adjacent to perivascular cuffs (data not shown).

Regional and Serial Distribution of BDV N Protein and Genomic RNA. Immunohistochemistry revealed N protein in brain of all infected but no control rats. At 2 wk p.i., N was localized to nuclei and cytoplasm of neurons and glial cells. Beginning at 3 wk, N was distributed diffusely in neuropil. All areas of Hc, including granule cells of DG, contained N from 2 wk. In Cblm, Purkinje cells stained as early as 2 wk; however, only a small proportion of astrocytes and Bergmann glia were infected, and neither microglia nor cerebellar granule cells showed signs of infection. Microglia did not stain in Hc or DG. In thymus, spleen, and liver, immunohistochemistry re-

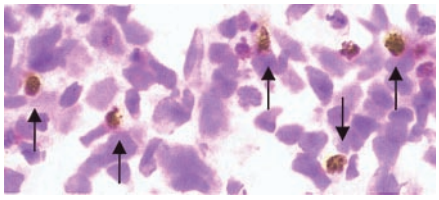

Fig. 8. Neuronal apoptosis in DG of neonatally infected rat at 4 wk p.i. TUNEL with hematoxylin counterstain. Labeled granule cells (arrows). (×400.)

vealed no staining at 2 wk, moderate staining at 4 wk, and marked staining at 6 wk. Viral protein was limited to nerve fibers in these tissues; only rarely were infected cells noted in splenic or thymic parenchyma. In NBD rats, BDV RNA was widespread in anterior portions of brain at 2 wk and increased in intensity and distribution through 24 wk p.i. BDV RNA was not detected in NL rats. BDV RNA was apparent at 2 wk in laminae I-II of Cx, cingulate Cx, septum, fornix, stria terminalis, dorsal endopiriform nucleus, habenula, CA1–CA3 and DG of Hc, Amyg, piriform Cx, parafascicular thalamic nucleus, anterior pretectal nucleus, and area postrema. Only light signal was seen in striatum, most of thalamus, hypothalamus, and cerebellar Cx until 6 wk p.i. At 4 wk, BDV RNA was readily detected in lamina II of Cx, claustrum, locus ceruleus, superior colliculi, pons, medial central gray, oculomotor and medial geniculate neurons, ventral tegmental area, and superior olivary and periolivary nuclei. BDV RNA was detected after 6 wk in retrosplenial aspects of frontal and temporal Cx, medial and ventral olfactory neurons, nucleus accumbens, raphe nucleus, substantia nigra, entorhinal Cx, uncinate fasciculus, and ventral cochlear nucleus.

TUNEL. TUNEL-labeled cells were present in cerebral Cx, DG, granule cell and molecular layer of Cblm, and periventricular germinal layers (Fig. 8; Table 2). The largest numbers of TUNEL-positive cells were found between 4 and 6 wk p.i. Most of the positive cells were apoptotic neurons, corresponding to damaged neurons observed in adjacent hematoxylin and eosin-stained sections; however, some lymphocytes in the inflammatory infiltrates were positive at 4 wk.

Discussion

We have identified neurobehavioral and motor disturbances that correlate temporally with shifts in soluble factor gene expression and neuropathology in a small animal model of neonatal infection and that parallel functional and anatomic neuropathology reported in autism and related neurodevelopmental disorders. Behavioral abnormalities include asymmetries in motor responses, aberrant righting reflexes, growth delay, dysregulated exploratory activity, and stereotypic behaviors. Histopathology is remarkable for microglial and astrocytic activation and neuronal apoptosis. These findings coincide with maximal gene expression of proinflammatory cytokines and apoptosis-related products. Inflammatory infiltrates are found transiently in Cx; however, their significance is unclear, as some behavioral disturbances antedate their appearance and infiltrates are not present in DG and Cblm, the two structures most severely damaged in this system.

Table 2. Frequency and regional distribution of TUNEL-positive cells

Group	Periventricular germinal layer	DG	Granular layer of Cblm	Cerebral Cx
4 wk NBD	12	30	16	66
4 wk NL	1	0	0	3
6 wk NBD	7	10	14	6
6 wk NL	0	0	0	4

Data are counts per region (hemisection of 20-μm coronal sections).

Apoptosis is not typically observed in normal rodent hippocampus beyond postnatal day 10 (34). In NBD rats, apoptosis continues to at least 6 wk p.i. Neuronal apoptosis in rabies precedes evidence of immune activation and is considered a direct, virus-induced event (35, 36). Likewise, the neuronal apoptosis observed in NBD rats occurs predominantly in Hc and Cblm, regions where inflammatory infiltrates are minimal or absent, and continues after resolution of cortical inflammation. Potential triggers for apoptotic cell loss in NBD rats include viral modulation of apoptosis-related products and proinflammatory cytokine gene expression. The peak of TUNEL labeling of neurons coincides with the peak at 4 wk p.i. of up-regulated gene expression of the pro-apoptotic Fas and caspase-1, down-regulation of mRNA for the anti-apoptotic bcl-x, and up-regulation of mRNA for the proinflammatory IL1α and -β, IL6, and TNFα. In other systems, withdrawal of neurotrophic factors may result in apoptosis. Although selected neurotrophic factor mRNAs are decreased in NBD rats, the regional and temporal expression of these changes is not consistent with a role in induction of apoptosis. Significant down-regulation of βNGF, BDNF, and NT3 mRNA is not observed before wk 12 and is restricted to Hc. Expression of the pro-apoptotic cytokine TNFβ correlates temporally with apoptosis in Cblm and prefrontal Cx: in Cblm, TNFβ mRNA levels and apoptosis are high at wk 6 and recede by wk 12; in prefrontal Cx, TNFβ mRNA levels and apoptosis diminish earlier (wk 6). Another potential factor in promotion of apoptosis, inducible NO synthase (37), is limited in distribution to perivascular infiltrates at the peak of inflammation and is unlikely to contribute to widespread neuronal loss. Susceptibility of neuronal populations to apoptosis after infection may depend on maturational differences in developmental programs influencing apoptosis (e.g., proliferative capacity, ref. 38; bcl-2/bax ratios, ref. 33; glutamate/*N*-methyl-D-aspartate receptors, ref. 39; adrenal steroids, ref. 39; protein kinase C, ref. 40; and cytokines, ref. 41), as presence of virus alone cannot account for the patterns of cell death observed.

A likely source of up-regulated proinflammatory cytokine gene expression is activated microglial cells or reactive astrocytes (42). The peak of cytokine mRNA changes at 4 wk corresponds to the appearance of prominent proliferation and activation morphology of microglial cells and modest increases in numbers of activated astrocytes. Interestingly, no microglia and only rare astrocytes appear to be infected. Thus, the mechanism of glial activation in NBD rats is likely to be indirect.

The occurrence of perivascular infiltrates at 4 wk p.i. parallels, but does not follow, either the up-regulation of proinflammatory cytokine gene expression throughout the brain or the appearance of viral antigen in nerve fibers of peripheral lymphoid organs (thymus, spleen). T cells in the infiltrates are distributed approximately equally between $CD4^+$ and $CD8^+$ subsets; however, preliminary cytotoxic T lymphocyte assays and studies of thymectomized rats indicate that these T cells are neither specific for BDV antigens nor integral to the damage seen in DG, Cblm, or Cx (unpublished results). Low levels of activated T cells can enter CNS independent of antigen specificity (43) or through normal recirculation through CNS without activation (44); nonetheless, priming by specific antigen is considered essential to retention of leukocytes in CNS through up-regulation of proinflammatory cytokines, adhesion molecules on endothelial cells, and chemokines (44). Whether BDV enhances leukocyte retention signals in selected brain regions, causing accumulation of lymphocytes in Cx without specifically activating T cells, is unclear. However, the nearly complete exclusion of mononuclear infiltrates from DG and Cblm is inconsistent with this hypothesis. An alternative explanation may relate to the neurodevelopmental time course for regional expression of factors such as adhesion molecules or chemokines. Indeed, susceptibility to encephalitogenic effects of Semliki Forest virus (45) or encepha-

lomyocarditis virus (46) during development is thought to depend more on maturity of Hc and Cblm than of immune responses.

Our finding of inflammatory infiltrates in Cx is similar to a recent report (47) of up-regulation of proinflammatory cytokines in neonatally infected rats in conjunction with transient immune infiltration and marked morbidity and mortality. However, our NBD rats had no mortality and did not manifest classical Borna disease. Instead, clinical assessments of NBD rats revealed only subtle signs of CNS dysfunction (minimally disheveled fur and dystonic postures, mild lethargy). Pilot studies indicate a more adult pattern of CNS disease when rats are inoculated after 12 h of postnatal life or with lower-titer stocks.

Evidence of growth retardation and dysfunction of locomotor development is present as early as day 4 p.i., precedes the advent of cytokine and glial activation, and suggests the possibility of direct virus-mediated effects on developing neural circuitry. Other CNS viral infections are associated with growth delay (48). Hypophagic effects of CNS or systemic infections are linked to increases in IL1, may be potentiated by TNFα, and likely act through area postrema (49), a circumventricular region involved in control of food and salt intake (50). Cells in area postrema are infected as early as 2 wk p.i.; however, cytokine mRNA levels were not measured in brainstem structures. Localized increases in IL1 or TNFα could contribute to decreased food intake and subsequent weight loss after neonatal infection; alternatively, direct viral effects may be responsible. The role of area postrema in regulating salt intake is of interest, given the salt preference described in NBD rats (9). Most intriguingly, the early protoambulatory asymmetries and deviant righting reflexes found in NBD rats are akin to abnormalities recently described in autism (51). Presumably, such dysfunction results from faulty cerebellar and striatal inputs in early stages of infection; however, viral signal in these structures is scant at 2 wk p.i. and cytokine mRNA levels do not peak in Cblm until 4 wk. Alternatively, direct or indirect viral influences may induce selective damage to neurotransmitter systems with relevance for motor function; in adult Borna disease, for example, loss of cholinergic innervation to Hc and Cx is reported as early as day 6 p.i. (52).

Behavioral disturbances of NBD rats parallel such clinical aspects of autism as stereotypies (14), abnormal unfolding of developmental motor milestones (51), and inhibited responses to novel stimuli (14). Although neuropathologic studies of autism are limited, reports of Purkinje and granule cell loss in Cblm (16) also suggest overlap with this neonatal infection paradigm. Epidemiologic associations of BDV with a plethora of human neuropsychiatric diseases remain controversial (53). Our blood studies of 61 children with autism do not show evidence of BDV infection (unpublished results). Nonetheless, similarities in behavioral and anatomic pathology in autism and NBD suggest the utility of the NBD model for defining common pathways for dysregulation of developmental programs and assessing the time course of vulnerability of discrete glial and neuronal populations to perturbations in cytokines, neurotrophins, and other soluble factors.

We thank M. Solbrig for valuable comments and M. Chatard, L. O'Rourke, and B. Bauder for technical assistance. This work was supported by National Institutes of Health Grants K08-MH01608 (M.H.) and NS29425 (W.I.L.); the Cure Autism Now Foundation and the National Alliance for Autism Research (W.I.L.); and the Austrian Fund for the Advancement of Scientific Research (H.W.).

1. Yolken, R. H. & Torrey, E. F. (1995) *Clin. Microbiol. Rev.* **8,** 131–145.
2. Hoek, H. W., Brown, A. S. & Susser, E. (1998) *Soc. Psychiatry Psychiatr. Epidemiol.* **33,** 372–379.
3. Nelson, K. B., Dambrosia, J. M., Grether, J. K. & Phillips, T. M. (1998) *Ann. Neurol.* **44,** 665–675.
4. Wyatt, R. J. (1996) *Arch. Gen. Psychiatry* **53,** 11–15.
5. Solbrig, M. V., Koob, G. F., Fallon, J. H. & Lipkin, W. I. (1994) *Neurobiol. Dis.* **1,** 111–119.
6. Rubin, S. A., Bautista, J. R., Moran, T. H., Schwartz, G. J. & Carbone, K. M. (1999) *Dev. Brain Res.* **112,** 237–244.
7. Bautista, J. R., Rubin, S. A., Moran, T. H., Schwartz, G. J. & Carbone, K. M. (1995) *Dev. Brain Res.* **90,** 45–53.
8. Narayan, O., Herzog, S., Frese, K., Scheefers, H. & Rott, R. (1983) *J. Infect. Dis.* **148,** 305–315.
9. Bautista, J. R., Schwartz, G. J., de la Torre, J. C., Moran, T. H. & Carbone, K. M. (1994) *Brain Res. Bull.* **34,** 31–40.
10. Pletnikov, M. V., Rubin, S. A., Vasudevan, K., Moran, T. H. & Carbone, K. M. (1999) *Behav. Brain Res.* **100,** 43–50.
11. Rubin, S. A., Sylves, P., Vogel, M., Pletnikov, M., Moran, T. H., Schwartz, G. J. & Carbone, K. M. (1999) *Brain Res. Bull.* **48,** 23–30.
12. Dittrich, W., Bode, L., Ludwig, H., Kao, M. & Schneider, K. (1989) *Biol. Psychiatry* **26,** 818–828.
13. Gillberg, C., Steffenburg, S. & Schaumann, H. (1991) *Brit. J. Psychiatry* **158,** 403–409.
14. Rapin, I. (1997) *N. Engl. J. Med.* **337,** 97–104.
15. Minshew, N. J. & Dombrowski, S. M. (1994) in *The Neurobiology of Autism,* eds. Bauman, M. L. & Kemper, T. L. (Johns Hopkins Univ. Press, Baltimore), pp. 66–85.
16. Bailey, A., Luthert, P., Dean, A., Harding, B., Janota, I., Montgomery, M., Rutter, M. & Lantos, P. (1998) *Brain* **121,** 889–905.
17. Bauman, M. L. & Kemper, T. L. (1994) in *The Neurobiology of Autism,* eds. Bauman, M. L. & Kemper, T. L. (Johns Hopkins Univ. Press, Baltimore), pp. 119–145.
18. Gillberg, C. (1990) *Acta Psychiatr. Scand.* **82,** 152–156.
19. Chess, S. (1971) *J. Autism Child. Schizophr.* **1,** 33–47.
20. Todd, R. D. (1986) *Psychiatr. Dev.* **2,** 147–165.
21. Warren, R. P. (1998) *CNS Spectrums* **3,** 71–79.
22. Anderson, G. M. (1994) in *The Neurobiology of Autism,* eds. Bauman, M. L. & Kemper, T. L. (Johns Hopkins Univ. Press, Baltimore), pp. 227–242.
23. Carbone, K. M., Duchala, C. S., Griffin, J. W., Kincaid, A. L. & Narayan, O. (1987) *J. Virol.* **61,** 3431–3440.
24. Altman, J. & Sudarshan, K. (1975) *Anim. Behav.* **23,** 896–920.
25. MacLennan, A. J. & Maier, S. F. (1983) *Science* **219,** 1091–1093.
26. Hickey, W. F., Gonatas, N. K., Kimura, H. & Wilson, D. B. (1983) *J. Immunol.* **131,** 2805–2809.
27. Gavrieli, Y., Sherman, Y. & Ben-Sasson, S. A. (1992) *J. Cell Biol.* **119,** 493–501.
28. Paxinos, G. & Watson, C. (1986) *The Rat Brain in Stereotaxic Coordinates* (Academic, San Diego).
29. Chomczynski, P. (1993) *BioTechniques* **15,** 532–537.
30. Lipkin, W. I., Travis, G., Carbone, K. & Wilson, M. (1990) *Proc. Natl. Acad. Sci. USA* **87,** 4184–4188.
31. Armitage, P. (1971) *Statistical Methods in Medical Research* (Blackwell Scientific, Oxford).
32. Siegel, S. (1956) *Nonparametric Statistics for the Behavioral Sciences* (McGraw-Hill, New York).
33. Gillardon, F., Zimmermann, M., Uhlmann, E., Krajewski, S., Reed, J. C. & Klimaschewski, L. (1996) *J. Neurosci. Res.* **43,** 726–734.
34. Toth, Z., Yan, X. X., Haftoglou, S., Ribak, C. E. & Baram, T. Z. (1998) *J. Neurosci.* **18,** 4285–4294.
35. Fu, Z. F., Weihe, E., Zheng, Y. M., Schäfer, M. K.-H., Sheng, H., Corisdeo, S., Rauscher, F. J., III, Koprowski, H. & Dietzschold, B. (1993) *J. Virol.* **67,** 6674–6681.
36. Theerasurakarn, S. & Ubol, S. (1998) *J. Neurovirol.* **4,** 407–414.
37. Fontana, A., Constam, D., Frei, K., Koedel, U., Pfister, W. & Weller, M. (1996) in *Cytokines and the CNS,* eds. Ransohoff, R. M. & Benveniste, E. N. (CRC, Boca Raton, FL), pp. 187–219.
38. Howard, M. K., Burke, L. C., Mailhos, C., Pizzey, A., Gilbert, C. S., Lawson, W. D., Collins, M. K., Thomas, N. S. & Latchman, D. S. (1993) *J. Neurochem.* **60,** 1783–1791.
39. Gould, E. & McEwen, B. S. (1993) *Curr. Opin. Neurobiol.* **3,** 676–682.
40. Barrios, M. & Liljequist, S. (1996) *Brain Res. Dev. Brain Res.* **94,** 22–30.
41. Mehler, M. F. & Kessler, J. A. (1997) *Trends Neurosci.* **20,** 357–365.
42. Benveniste, E. N. (1997) in *Immunology of the Nervous System,* eds. Keane, R. W. & Hickey, W. F. (Oxford Univ. Press, New York), pp. 419–459.
43. Hickey, W. F. (1991) *Brain Pathol.* **1,** 97–105.
44. Seabrook, T. J., Johnston, M. & Hay, J. B. (1998) *J. Neuroimmunol.* **91,** 100–107.
45. Oliver, K. R., Scallan, M. F., Dyson, H. & Fazakerley, J. K. (1997) *J. Neurovirol.* **3,** 38–48.
46. Ikegami, H., Takeda, M. & Doi, K. (1997) *Int. J. Exp. Pathol.* **78,** 101–107.
47. Sauder, C. & de la Torre, J. C. (1999) *J. Neuroimmunol.* **96,** 29–45.
48. Pollack, H., Kuchuk, A., Cowan, L., Hacimamutoglu, S., Glasberg, H., David, R., Krasinski, K., Borkowsky, W. & Oberfield, S. (1996) *Brain Behav. Immunity* **10,** 298–312.
49. Dantzer, R., Bluthé, R.-M., Layé, S., Bret-Dibat, J.-L., Parnet, P. & Kelley, K. W. (1998) *Ann. N.Y. Acad. Sci.* **840,** 586–590.
50. Wang, T. & Edwards, G. L. (1997) *Am. J. Physiol.* **273,** R1290–R1308.
51. Teitelbaum, P., Teitelbaum, O., Nye, J., Fryman, J. & Maurer, R. G. (1998) *Proc. Natl. Acad. Sci. USA* **95,** 13982–13987.
52. Gies, U., Bilzer, T., Stitz, L. & Staiger, J. F. (1998) *Brain Pathol.* **8,** 39–48.
53. Lipkin, W. I., Schneemann, A. & Solbrig, M. V. (1995) *Trends Microbiol.* **3,** 64–69.